Microfluid Nanofluid (2014) 17:821–829
DOI 10.1007/s10404-014-1372-4

RESEARCH PAPER

A massively parallel microfluidic device for long-term visualization of isolated motile cells

Shakked O. Halperin · Chelsey T. Poling · Shilpi R. Mathrani · Brendan W. Turner · Adrienne C. Greene · Megan E. Dueck · Frank B. Myers

Received: 23 April 2013 / Accepted: 24 February 2014 / Published online: 14 March 2014

Abstract Visualizing the natural behavior of motile cells over many hours is a challenge, as cells can leave the field of view of a microscope in a matter of minutes. Many interesting cell behaviors—such as cell division, motility phenotype, cell–cell interactions, and multicellular colony formation—require hours of observation to characterize. We present a microfluidic device that traps hundreds of single motile cells in isolated chambers, thereby allowing observation over several days. This polydimethylsiloxane device features 400 circular chambers, connected to a central serpentine channel. Motile cells are loaded into these chambers through the serpentine channel. The channel is then purged with air, fluidically isolating the chambers from each other and effectively trapping the cells. We applied the device to observe the behavior of the choanoflagellate *Salpingoeca rosetta*. Because of its ability to live in both solitary and colonial forms, *S. rosetta* is a useful model organism for the study of the evolutionary origins of multicellularity. In particular, *S. rosetta* can take on two distinct colonial forms: chain colonies and rosette colonies. With our device, we are able to observe the formation of these colonies from single cells more easily and with higher throughput than ever before. This device has the potential to be a powerful tool for studying the long-term behavior of motile cells.

Keywords Microfluidic · Motile · Choanoflagellate · Isolation · Visualization · Cell

1 Introduction

Microfluidic biological assays allow investigators to address biological questions which are difficult to answer with conventional techniques. With microfluidic trapping technologies, single-cell assays can be performed in a high-throughput manner using limited reagents (Breslauer et al. 2006; Ingham and Vlieg 2008; Kim et al. 2008; Muralimohan et al. 2009; Nilsson et al. 2009; Weibel et al. 2007; Di Carlo and Lee 2006). Along with this advantage, microfluidic has also made it possible to grow cells indefinitely within a chemostat (Balaban 2005; Groisman et al. 2005; Novick and Szilard 1950), study cellular

Shakked O. Halperin and Chelsey T. Poling have contributed equally.

Electronic supplementary material The online version of this article (doi:10.1007/s10404-014-1372-4) contains supplementary material, which is available to authorized users.

S. O. Halperin · C. T. Poling · B. W. Turner · A. C. Greene · M. E. Dueck · F. B. Myers
Biology-on-a-Chip Internship Program REU, University of California, Berkeley, Berkeley, CA, USA

S. O. Halperin
Department of Biological Engineering, University of Missouri, Columbia, MO, USA

C. T. Poling
School of Biological and Health Systems Engineering, Arizona State University, Tempe, AZ, USA

S. R. Mathrani · B. W. Turner · F. B. Myers (✉)
Department of Bioengineering, University of California, Berkeley, 121 Stanley Hall, Berkeley, CA 94720, USA
e-mail: fbm@berkeley.edu

A. C. Greene
Department of Molecular and Cell Biology, University of California, Berkeley, Berkeley, CA, USA

M. E. Dueck
Department of Biology, University of California, San Diego, La Jolla, CA, USA

chemotaxis with a steady-state concentration gradient (Mao et al. 2003), and allow cell sorting and sample dispensing all on one chip (Fu et al. 2002), to name a few examples.

The choanoflagellate *Salpingoeca rosetta* is a flagellated protozoan whose study would greatly benefit from an effective microfluidic isolation device. Choanoflagellates are the closest known extant relatives of metazoans (Fairclough et al. 2010; King 2004, 2005; Lang et al. 2002). *S. rosetta* is a unique model organism for studying the evolution of multicellularity because it can exist either solitarily or in one of two colonial forms, chain or rosette, depending on environmental cues (Alegado et al. 2012; Fairclough et al. 2010). Visualizing the formation of *S. rosetta* colonies from a single cell using conventional techniques is an extremely time-consuming and challenging task, as it requires constant tracking of the cells for at least 12 h. Furthermore, it is difficult to track more than one cell/colony at a time. Long-term visualization would be more accessible with the aid of a high-throughput microfluidic device that could isolate single cells within one microscopic field of view without hindering their movement.

Designing such an isolation device presents several challenges. Most microfluidic devices for single-cell analysis are designed for adherent cells with limited motility. Motile cells, such as choanoflagellates, are capable of escaping most device traps. Microwells, for example, are effective with adherent cells for a wide range of applications (Lindstrom and Andersson-Svahn 2010, 2011) including studying the dynamics of stem cell differentiation (Lindstrom et al. 2009a), massively multiplexed PCR genotyping (Lindstrom et al. 2009b), and protein-binding assays (Friedman et al. 2009); however, microwells cannot confine cells in 3D, and so motile cells can simply swim out of the chambers (Lindstrom and Andersson-Svahn 2011). Another common method for studying non-motile cells is a mechanical trap, which confines cells with a variety of different physical structures. Examples of the diverse techniques developed for mechanical traps include using magnetic force to immobilize cells into an array (Liu et al. 2009), capturing large cells by filtering cell solution through a membrane microfilter (Zheng et al. 2007), and trapping single cells within *U*-shaped structures (Di Carlo et al. 2006). However, even if these traps could be adapted for use with motile cells, they ultimately immobilize the cells, thereby preventing the study of their natural movement and behavior. The few devices that have been specifically designed for motile cells similarly immobilize the cells using hydrodynamic trapping (Kumano et al. 2012; Lutz et al. 2006), likewise rendering these devices inadequate for studying cell motility, growth, or developmental processes. Clearly, a need exists for a device that can be used for visualization of motile cells without hindering their movement or subjecting them to mechanical forces that may alter their behavior.

We present a microfluidic device that traps single motile *S. rosetta* cells in isolated chambers where cells can function normally and move freely. Each chamber serves as a miniaturized suspension cell culture for the isolated motile cells. The cells can be visualized for over 65 h as they divide, form colonies, and interact with other daughter cells. The design is both simple to fabricate and simple to operate. The chip consists of 400 circular chambers, branching off of a serpentine channel and can be self-loaded with the cell solution after vacuum treatment by degas-driven flow (Cira et al. 2012; Dimov et al. 2011; Luo et al. 2008). Degas-driven flow is a simple loading mechanism that is caused by the diffusion of air back into PDMS after the device has been 'degassed' in a vacuum. As the PDMS absorbs the air, this creates negative pressure inside the channels of the device, which draws the sample fluid into the isolation chambers. The chip can be vacuum-treated just prior to an experiment. Alternatively, if a vacuum system is unavailable in the laboratory, the chips can be pretreated with vacuum at the time of fabrication and hermetically sealed in plastic bags with an inexpensive food vacuum sealer. In that case, the bag is simply cut open and the chip immediately loaded with the cell solution. After loading the cell solution, the chambers are fluidically isolated by pumping air through the serpentine channel, creating an air–fluid barrier that effectively traps the cells in the chambers. Surface tension at the narrow chamber opening prevents the media in the chambers from being flushed out during this process. Once the cells are confined, we can observe cell behavior, division, and colony formation on a massive scale unattainable with conventional techniques.

Media retention, chamber size parameters, and cell media concentration have all been optimized for the study of *S. rosetta*, but can easily be modified for application to other types of motile organisms. This device provides a simple and high-throughput way to study the division and interaction of motile microorganisms through long-term visualization.

2 Methods

2.1 Device fabrication

We fabricated the microfluidic device using standard soft lithography (Xia et al. 1999). A 50-μm single-layer negative mold was photolithographically patterned with SU-8 photoresist. Polydimethylsiloxane (PDMS, Sylgard 184), mixed at a 10:1 elastomer-to-curing-agent ratio, was

poured over the mold and allowed to cure for 4 h at 60 °C. PDMS devices were bonded to a glass slide via oxygen plasma treatment. The devices included 400 trapping chambers, 70 μm in radius, connected to a 60-μm-wide serpentine channel via media retention bridges, 70 μm long and 25 μm wide (Fig. 1).

2.2 Microfluidic device operation

The choanoflagellate suspension was loaded via degas-driven flow, and the chambers were then isolated by flowing air through the serpentine channel (Fig. 2). First, we placed the device in a vacuum chamber for ten min at ~300 mTorr with the outlet hole covered with Scotch tape (3 M). After removing the device from the vacuum, 20 μL of cell suspension was placed on the inlet. After 30 min, media had entirely filled the chambers, and cells were distributed among the chambers (Online Resource 1). We removed the tape covering the outlet and inserted a stainless steel catheter into the outlet hole. A 10-mL syringe on a syringe pump (New Era Pump Systems) was connected with tubing to the inlet hole of the device with a stainless steel catheter. Since PDMS is permeable to water vapor, the device was completely submerged in a petri dish filled with deionized water to prevent media evaporation from the chambers. The syringe pump pumped air through the device at 10 mL/h until the loading channel had been evacuated (Online Resource 2). Once the loading channel was evacuated, the syringe pump was set to 0.1 mL/h for the remainder of the study. This constant airflow provided necessary oxygen transport to support cell viability.

2.3 Cell culture

The choanoflagellate cell line *S. rosetta* (ATCC) with *E. pacifica* bacteria was cultivated in cereal grass media, which is processed by steeping artificial sea water in Ward's cereal grass (Scholar Chemistry), followed by filter sterilizing. The cells were grown at room temperature and subcultured every 1–2 days.

In preparation for cell injection into the microfluidic chip, cells were subcultured daily at a 1:5 cell-to-media concentration to progress the cells into log-phase growth. We concentrated the cells by centrifugation, followed by aspiration of the media. To form rosette colonies, one colony of *A. machipongonensis* was added to the cells. Since the culture was still dominantly composed of single cells up to 18 h after induction, we waited approximately 12–18 h before loading the induced cells into the chip.

2.4 Visualization of cells on chip

Cells were visualized on the chip under phase-contrast microscopy. For long-term visualization of a small number of chambers, one field of view of the microscope was recorded for 24 h with images taken at 10-s intervals. For experiments involving many chambers, an automated stage was used to take pictures of each chamber in the device once per hour for 68 h. ImageJ was used to conduct particle tracking of the cells in the chambers, and MATLAB was used to process the data from ImageJ.

2.5 Media retention analysis

Media retention capabilities of submerged and non-submerged devices were examined with a fluorescence-based assay. After loading the devices with a 1 μM solution of green fluorescent protein (GFP) in deionized water, we submerged one device in a petri dish filled with water and left another device non-submerged. We evacuated the serpentine channels of the devices, leaving GFP only inside the chambers, and imaged three consecutive rows of each device at 0, 3, 6, 12, and 24 h after evacuating the serpentine channel. The images were captured using an

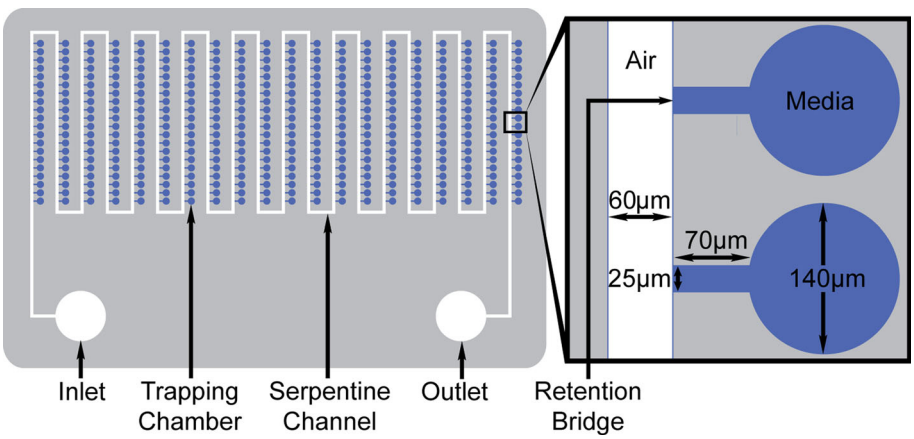

Fig. 1 The device consists of 400 trapping chambers branching from a serpentine channel. Narrow retention bridges between the chambers and the serpentine channel decrease media loss in the circular viewing chambers. Air is pumped through the serpentine channel to achieve fluidic isolation of each chamber

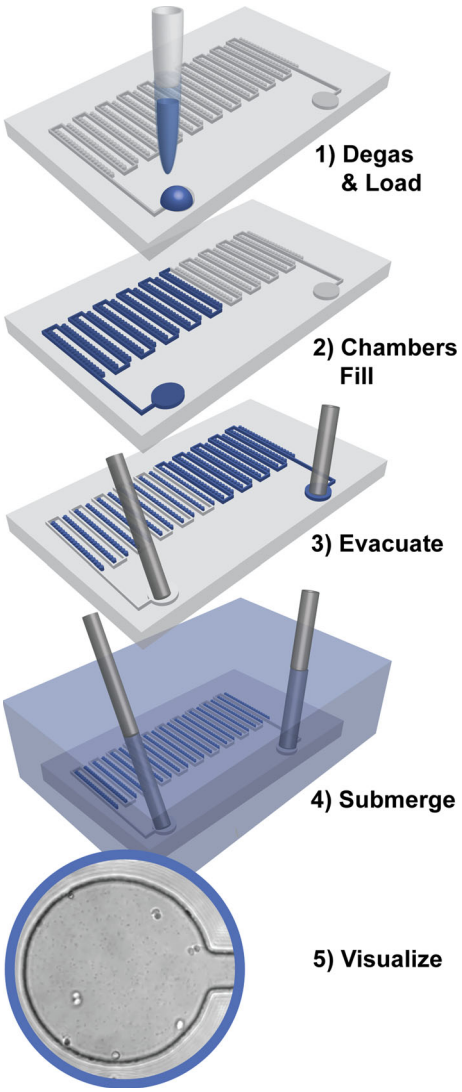

Fig. 2 To operate, the device is degassed in a vacuum chamber for 5 min (*1*). After removal from the vacuum chamber, a drop of cell solution is loaded on the inlet, which fills all the chambers (*2*). Next, a syringe pump flows air through the device evacuating the serpentine channel and effectively trapping the cells in the chambers (*3*). Finally, the device is submerged in water to retain media (*4*). The cells can then be visualized under a microscope (*5*)

inverted epi-fluorescence microscope with a 40× objective magnification (Motic AE31). The cross-sectional area of media retained was determined across >20 chambers at each time point using ImageJ.

2.6 Chamber size comparison

Three different devices were fabricated with chambers of 30, 50, and 70 μm radii to investigate the effect of chamber size on the rate of proliferation of trapped cells. A cell suspension containing 2.5×10^6 cells/mL of media was injected into the chip and loaded into the three different devices simultaneously. Cell numbers were recorded in each chamber of five rows for each device at 0, 12, and 24 h after loading.

2.7 Trapping efficiency analysis

The distribution of the number of trapped cells per chamber given different cell concentrations was analyzed. The device was loaded with four different concentrations of choanoflagellates in media, ranging from 100,000 cells/mL to 8.35 million cells/mL. To allow the cells to become more evenly distributed across the device, cells were allowed to move naturally for 30 min after loading the devices, before counting began. After the incubation, the number of cells in each trapping chamber from four rows of the device was recorded.

3 Results and discussion

3.1 Visualization of cells on chip

We were able to visualize the *S. rosetta* cells in the device under phase contrast for over 2 days as they moved throughout the chambers, interacted with each other, proliferated, and formed colonies.

Figure 3a shows a rosette colony that formed in the device from a single cell after induction with *A. machipongonensis* 18 h prior to loading. The image was captured 18 h after loading the device. Due to the extreme difficulty in using conventional methods to visualize motile cells, the formation of a rosette colony has been captured on video only once before (Fairclough et al. 2010). Our device has the potential to procure hundreds of recordings of rosette formations within a single experiment. Figure 3b demonstrates tracking of several

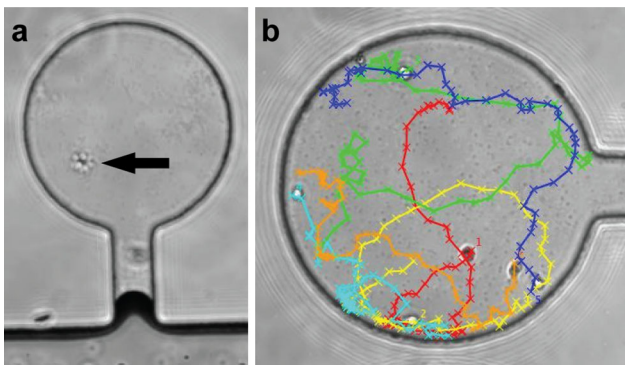

Fig. 3 **a** Phase-contrast image of a rosette colony that formed in the device, starting from a single cell. **b** This *image* shows the path of several choanoflagellates in an isolated chamber over a short period of time. Each '*x*' represents the location of a cell after five frames of video (at 30 frames per second)

choanoflagellates in a chamber over a period of 10 s (Online Resource 3). Such tracking can enable high-throughput studies of motility phenotype.

Using an automated stage, we captured data from many chambers over a 68-h period. We investigated colony formation of *S. rosetta* cells by recording the percentage of cells which formed colonies versus those that remained solitary based on the proximity of neighboring cells. Eleven chambers which had a single, healthy cell at the start of the experiment were selected for analysis. Cells which had a centroid spacing within 10 μm of one another were considered to be part of a colony; all others were considered solitary.

After 68 h, the average cells per chamber had grown from 1 cell to 6.9 cells, corresponding to a doubling time of 21.4 h, which is within the range of doubling times of 11–25 h seen in bulk culture conditions (Wain 2011; Fairclough e al. 2010). This indicates that the device does not adversely affect cell proliferation. Approximately 25 h into the experiment, the average number of cells per chamber reached two, and the percentage of solitary cells decreased below 20 % as the cells began forming chain colonies (Fig. 4a, b). As the colonies increased in size, cells began to bud off the colonies, resulting in an increase in the percentage of solitary cells approximately 45 h after loading (Fig. 4b, c). One possible explanation for this observation is that colony size is limited by mass transport of nutrients, so beyond a certain size, colonies tend to disaggregate. Figure 4d shows representative images of one chamber at different time points illustrating a single starting cell (3 h), a chain colony of three cells (31 h), partial disaggregation of this colony as it grows to five cells (45 h), and complete disaggregation with seven cells in the chamber (67 h).

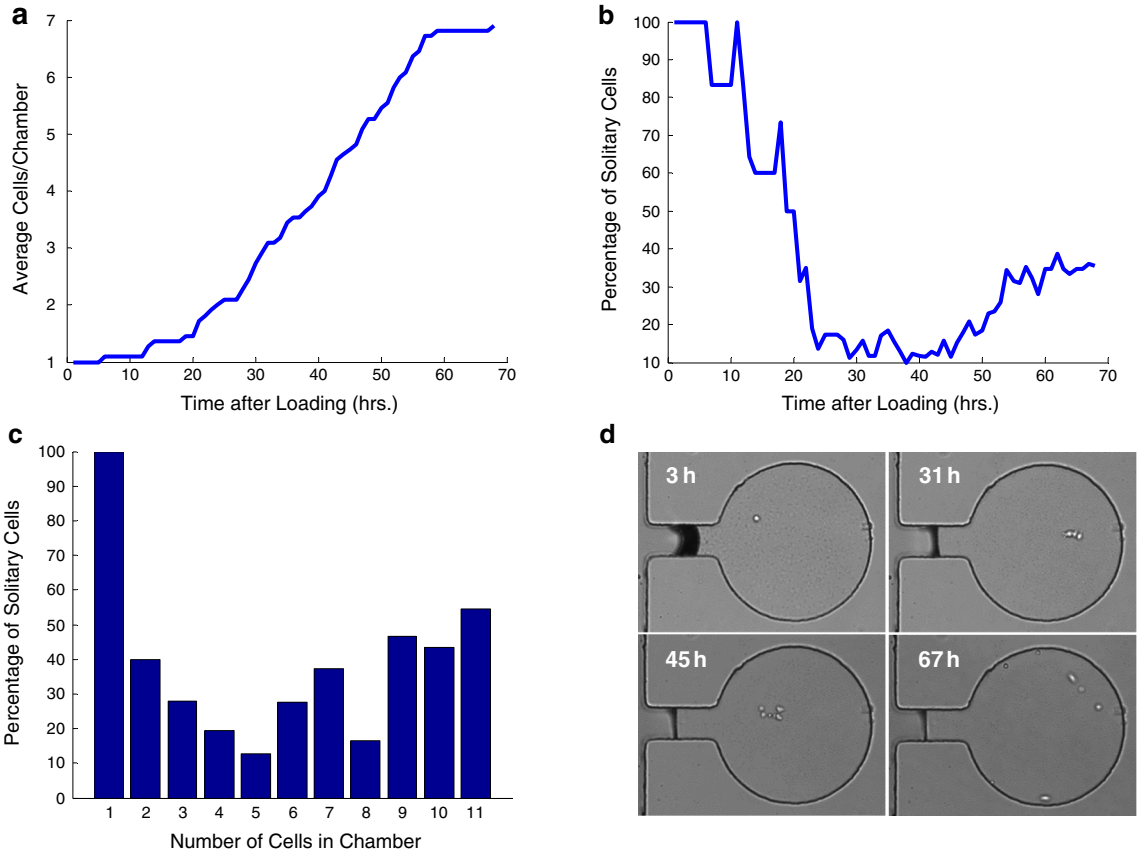

Fig. 4 **a** This *graph* shows the average number of cells per chamber across 11 selected chambers. **b** This *graph* shows the percentage of solitary cells over time. At the start of the experiment, each chamber had exactly one cell; therefore, all of the cells were in a solitary form. As the average cells/chamber increased, the cells began to form chain colonies, causing the percentage of solitary cells to fall. The percentage of solitary cells increase after 48 h, as cells begin to bud off the colonies. **c** This *graph* illustrates how the percentage of solitary cells vary depending on the number of cells in the chamber. From 1 to 5 cells per chamber, there is a sharp decrease in the number of solitary cells. As the chain colonies grow in size, cells begin to bud off, increasing the percentage of solitary cells. **d** Phase-contrast images of one chamber at four time points. At 3 h, a single cell is present in the chamber. The *images at 31 and 45 h* show that the cell has divided and begun forming a chain colony (with 3 and 5 cells, respectively). After 67 h, the number of cells in the chamber has grown to 7, and the colony has completely disaggregated. Full time-lapse of this chamber is available in Online Resource 5

3.2 Media retention analysis

Because PDMS is gas-permeable and microfluidic devices contain very small volumes of fluid, evaporation is a major concern. To address this issue, we submerged devices in a shallow dish of deionized water. This method substantially reduced media depletion due to evaporation and PDMS absorption. Even after 24 h, the submerged chips still had approximately 90 % of the GFP solution in the chambers, whereas the non-submerged chips had only 12 % of the solution remaining (Fig. 5).

Submerging the devices in water has proven to be an effective and simple means of retaining media in the trapping chambers, enabling long-term experiments. Retention of media is important not only for visualizing cells long term but also for maintaining the concentration of the media components, since solvent evaporation will lead to an increase in solute concentration. For short-term applications where the maintenance of solute concentration is of less concern, submerging might not be necessary. The retention bridge provides time to complete short-term experiments with non-submerged devices. Applying a previously developed algorithm (EPA 1999), we calculated a bridge retention time of 3.65 h, while our experiment showed depletion of bridge media after only 3 h ('Appendix'). We attribute the increased rate of media depletion to PDMS absorption of the media (Regehr et al. 2009).

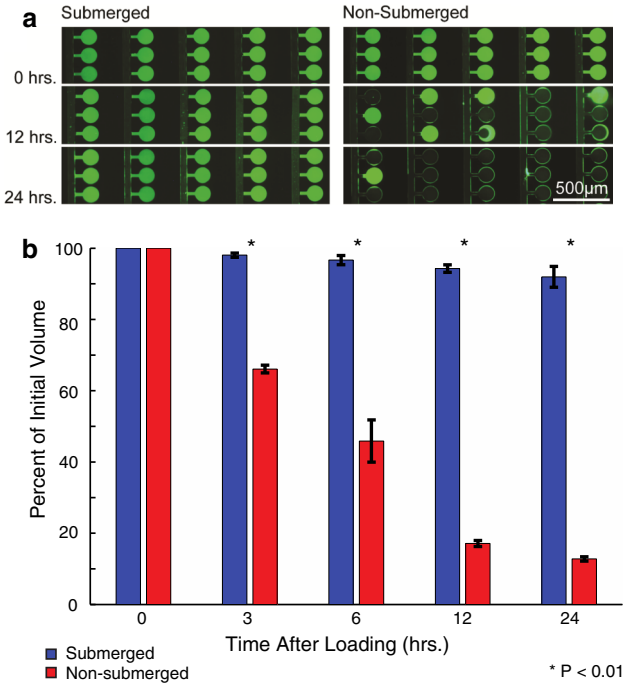

Fig. 5 **a** Epi-fluorescence photographs taken at 0, 12, and 24 h after evacuation of the serpentine channels demonstrate the effect of submerging the chip on media retention. In the submerged chip, little solution was lost after 24 h; however, the majority of the solution was lost in almost every chamber of the non-submerged chip after 24 h. **b** This *graph* shows the percent of the initial volume of GFP solution in the chambers after 3, 6, 12, and 24 h after loading. All values, obtained by image processing of epi-fluorescence photographs, represent the cross-sectional area of GFP solution retained in the chambers. The *blue bars* represent the submerged chips, while the *red bars* represent the non-submerged chips. After 24 h, the non-submerged chips lost approximately 88 % of the solution, nearly 8x more than the submerged chips (color figure online)

3.3 Chamber size comparison

We found a positive correlation between chamber size and the rate of proliferation (Fig. 6). For the smallest chambers with 30 μm radii, we observed no proliferation, even after 24 h. However, for chambers with 50 and 70 μm radii, after 24 h the number of cells increased by 30 and 50 %, respectively.

We propose that the significant effect chamber size has on proliferation can be attributed to nutrient consumption and interactions with the PDMS. Cell growth and division have been shown to be directly related to the cell media's nutrient condition and concentration (Umehara et al. 2003). By fluidically isolating the cells in a given amount of media, we are forming microecosystems with specific ratios of organisms to consumable nutrients. Since most chambers with choanoflagellates contain only one or two cells after loading (regardless of chamber radius), the larger volumes provide more nutrients for these cells and thus increase viability and potential growth rates. Additionally, PDMS oligomers are known to leech into microfluidic devices and adversely affect cell health (Regehr et al. 2009). Increasing the chamber size, thereby decreasing its surface-area-to-volume ratio, may reduce this effect.

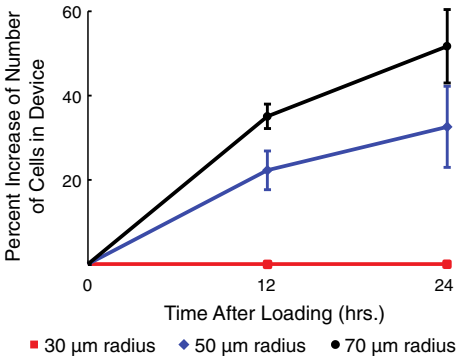

Fig. 6 This *graph* shows the percent increase in number of cells in the device for three different chamber sizes. The largest chambers of 70 μm radius showed the largest percent increase in cells, more than 50 % after 24 h. The 30-μm-radius chambers had no increase in cells, and the 50-μm-radius chambers had a 30 % increase

While the trend would suggest further increasing chamber size to increase cell proliferation, we chose 70 μm as an ideal radius because it allowed visualization of multiple chambers in one field of view while simultaneously yielding adequate proliferation. The specific chamber size needed for a given organism will depend on its specific nutrient consumption rate.

3.4 Trapping efficiency analysis

The distribution of cells in the devices varied based on the loaded cell concentration. At very low cell concentrations (100,000 and 500,000 cells/mL), most chambers had no cells, while less than 5 % had only one cell. At 2,500,000 cells/mL, over 80 % of the chambers were occupied by at least one cell, and nearly a third of the chambers had exactly one cell trapped inside. At the highest concentration of 8,350,000 cells/mL, almost every chamber was filled, but over 85 % had two or more cells inside.

We compared the distribution of cells in our device to a Poisson's distribution, which assumes that the cells act independently of one another (Fig. 7a); therefore, the trapping of one cell in a chamber neither increases nor diminishes the chance of another cell being trapped. Although the Poisson's model accurately predicts the general trend for the likelihood of a chamber containing 0, 1, or >2 cells, it deviates in certain places, particularly in predicting the percentage of chambers with 1 or >2 cells. This is likely due to the fact that some cells load as clumps.

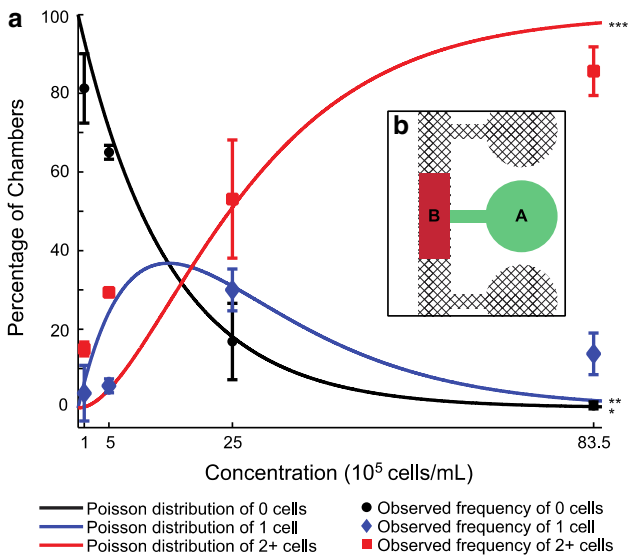

Fig. 7 **a** The observed frequencies of 0 cells/chamber, 1 cell/chamber, and 2+ cells/chamber are plotted against the expected Poisson's distribution for the four different concentrations that we tested. The Poisson's distribution provides a reasonable approximation of the distribution of trapped cells in the device. **b** The *green area* (labeled *a*) represents the trapping region, and the *red area* (labeled *b*) represents the non-trapping region. These areas are used for the equation to obtain the optimal concentration for a desired distribution of cells/chamber. The size and shape of these areas could be modified for different organisms and purposes (color figure online)

The following equation will provide the optimal concentration, assuming a Poisson's distribution, for obtaining the highest percentage of chambers with a desired distribution. We encourage the modification of our device for the specific organism of study; therefore, the equation will accommodate any changes in area, volume, or number of chambers in the device.

$$\text{Optimal concentration} = \frac{k(A+B)n}{AV}$$

k desired number of cells/chamber, A area of trapping region (Fig. 7), B area of non-trapping region (Fig. 7), V volume of device (mL), and n number of chambers.

4 Conclusion

Our novel microfluidic platform allows high-throughput visualization of the movement and behavior of motile cells for extended time periods. The device offers a number of advantages over conventional visualization methods, as well as similar microfluidic devices. The conventional method of visualizing cells in a petri dish is low throughput and requires constant tracking to keep the motile cell in the field of view of the microscope. Our easy-to-operate device confines cells to one of many chambers which can be individually observed using an automated stage. Unlike other devices designed for motile organisms, our device traps cells in a hydrostatic environment without immobilizing them, thereby allowing them to move and behave normally.

Our device can be used in a number of different ways. Depending on the study, it could be used either to visualize cells in a few chambers for a long time period or to image every chamber in the device using an automated stage in order to obtain large sample sizes. The number of chambers, as well as their shapes and sizes, may be tailored to particular experimental needs. We have provided equations for determining the evaporation time of media in the device and the optimal concentration of cells for a desired distribution, which will also aid in experiment design. We anticipate this platform finding many applications in the study of motile cell behavior.

Acknowledgments We would like to thank Nicole King, Terry Johnson, Arielle Woznica, and Tera Levin for their mentorship and guidance. We would also like to thank the King laboratory for graciously providing the *S. rosetta* cells. This work was supported by the National Science Foundation's Research Experience for Undergraduates (REU) program under Grant No. 0852058.

Appendix: Media retention equations

US EPA method

$$E = \frac{0.1288 \cdot A \cdot P \cdot M^{0.667} \cdot u^{0.78}}{T}$$

E evaporation rate (kg/min), u wind speed just above the pool liquid surface (m/s), M pool liquid molecular weight, A surface area of the pool liquid (m^2), P pool liquid vapor pressure at the pool temperature (kPa), T pool liquid absolute temperature (K).

Retention bridge evaporation time

$$t = t_{\text{evac}} + \frac{(2.21 \times 10^{11}) \cdot l_B \cdot T \cdot (w_s \cdot h)^{0.78}}{P \cdot M^{0.667} \cdot Q_s^{0.78}} - \frac{t_{\text{evac}} \cdot Q_{\text{evac}}^{0.78}}{Q_s^{0.78}}$$

t time for media in bridge to evaporate (min), t_{evac} time syringe pump set to Q_{evac} (min), l_B bridge length (m), T media absolute temperature (K), w_s serpentine width (m), h channel height (m), P vapor pressure of media at T (kPa), M media solvent molecular weight, QS study flow rate (mL/h), Q_{evac} serpentine evacuation flow rate (mL/h).

References

Alegado RA, Brown LW, Cao S, Dermenjian RK, Zuzow R, Fairclough SR, Clardy J, King N (2012) A bacterial sulfonolipid triggers multicellular development in the closest living relatives of animals. eLife. doi:10.7554/eLife.00013

Balaban NQ (2005) Szilard's dream. Nat Methods 2:648–649. doi:10.1038/nmeth0905-648

Breslauer DN, Lee PJ, Lee LP (2006) Microfluidics-based systems biology. Mol BioSyst 2:97–112. doi:10.1039/b515632g

Cira NJ, Ho JY, Dueck ME, Weibel DB (2012) A self-loading microfluidic device for determining the minimum inhibitory concentration of antibiotics. Lab Chip 12:1052–1059. doi:10.1039/c2lc20887c

Di Carlo D, Lee LP (2006) Dynamic single-cell analysis for quantitative biology. Anal Chem 78:7918–7925. doi:10.1021/ac069490p

Di Carlo D, Wu LY, Lee LP (2006) Dynamic single cell culture array. Lab Chip 6:1445–1449. doi:10.1039/B605937F

Dimov IK, Basabe-Desmonts L, Garcia-Cordero JL, Ross BM, Ricco AJ, Lee LP (2011) Stand-alone self-powered integrated microfluidic blood analysis system (SIMBAS). Lab Chip 11:845–850. doi:10.1039/c0lc00403k

EPA (1999) Risk management program guidance for offsite consequence analysis. U.S. EPA. EPA-550-B-99-009. http://daq.state.nc.us/toxics/risk/112r/files/guid_oca-all(31).pdf. Accessed 1 Nov 2012

Fairclough SR, Dayel MJ, King N (2010) Multicellular development in a choanoflagellate. Curr Biol 20:R875–R876. doi:10.1016/j.cub.2010.09.014

Friedman M, Lindstrom S, Ekerljung L, Andersson-Svahn H, Carlsson J, Brismar H, Gedda L, Frejd FY, Stahl S (2009) Engineering and characterization of a bispecific HER2 × EGFR-binding affibody molecule. Biotech Appl Biochem 54:121–131. doi:10.1042/BA20090096

Fu AY, Chou H, Spence C, Arnold FH, Quake SR (2002) An integrated microfabricated cell sorter. Anal Chem 74:2451–2457. doi:10.1021/ac0255330

Groisman A, Lobo C, Cho H, Campbell JK, Dufour YS, Stevens AM, Levchenko A (2005) A microfluidic chemostat for experiments with bacterial and yeast cells. Nat Methods 2:685–689. doi:10.1038/NMETH784

Ingham CJ, Vlieg JETVH (2008) MEMS and the microbe. Lab Chip 8:1604–1616. doi:10.1039/b804790a

Kim SM, Lee SH, Suh KY (2008) Cell research with physically modified microfluidic channels: a review. Lab Chip 8:1015–1023. doi:10.1039/b800835c

King N (2004) The unicellular ancestry of animal development. Dev Cell 7:313–325. doi:10.1016/j.devcel.2004.08.010

King N (2005) Choanoflagellates. Curr Biol 15:R113–R114. doi:10.1016/j.cub.2005.02.004

Kumano I, Hosoda K, Suzuki H, Hirata K, Yomo T (2012) Hydrodynamic trapping of *Tetrahymena thermophila* for the long-term monitoring of cell behaviors. Lab Chip 12:3451–3457. doi:10.1039/c2lc40367f

Lang BF, O'Kelly C, Nerad T, Gray MW, Burger G (2002) The closest unicellular relatives of animals. Curr Biol 12:1773–1778. doi:10.1016/S0960-9822(02)01187-9

Lindstrom S, Andersson-Svahn H (2010) Overview of single-cell analyses: microdevices and applications. Lab Chip 10:3363–3372. doi:10.1039/c0lc00150c

Lindstrom S, Andersson-Svahn H (2011) Miniaturization of biological assays—overview on microwell devices for single-cell analyses. Biochim Biophys Acta 1810:308–316. doi:10.1016/j.bbagen.2010.04.009

Lindstrom S, Eriksson M, Vazin T, Sandberg J, Lundeberg J, Frisen J, Andersson-Svahn H (2009a) High-density microwell chip for culture and analysis of stem cells. PLoS ONE 4:e6997. doi:10.1371/journal.pone.0006997

Lindstrom S, Hammond M, Brismar H, Andersson-Svahn H, Ahmadian A (2009b) PCR amplification and genetic analysis in a microwell cell culturing chip. Lab Chip 9:3465–3471. doi:10.1039/B912596E

Liu W, Dechev N, Foulds IG, Burke R, Parameswaran A, Park EJ (2009) A novel permalloy based magnetic single cell micro array. Lab Chip 9:2381–2390. doi:10.1039/b821044f

Luo C, Zhu X, Yu T, Luo X, Ouyang Q, Ji H, Chen Y (2008) A fast cell loading and high throughput microfluidic system for long-term cell culture in zero flow environments. Biotechnol Bioeng 101(1):190–195. doi:10.1002/bit.21877

Lutz BR, Chen J, Schwartz DT (2006) Hydrodynamic tweezers: 1. Noncontact trapping of single cells using steady streaming microeddies. Anal Chem 78:5429–5435. doi:10.1021/ac060555y

Mao H, Cremer PS, Manson MD (2003) A sensitive, versatile microfluidic assay for bacterial chemotaxis. Proc Natl Acad Sci 100:5449–5454. doi:10.1073/pnas.0931258100

Muralimohan A, Eun YJ, Bhattacharyya B, Weibel DB (2009) Dissecting microbiological systems using materials science. Trends Microbiol 17:100–108. doi:10.1016/j.tim.2008.11.007

Nilsson J, Evander M, Hammarstrom B, Laurell T (2009) Review of cell and particle trapping in microfluidic systems. Anal Chim Acta 649:141–157. doi:10.1016/j.aca.2009.07.017

Novick A, Szilard L (1950) Description of the chemostat. Science 112:715–716

Regehr KJ, Domenech M, Koepsel JT, Carver KC, Ellison-Zelski SJ, Murphy WL, Schuler LA, Alarid ET, Beebe DJ (2009) Biological implications of polydimethylsiloxane-based microfluidic cell culture. Lab Chip 9:2132–2139. doi:10.1039/B903043C

Umehara S, Wakamoto Y, Inoue I, Yasuda K (2003) On-chip single-cell microcultivation assay for monitoring environmental effects

on isolated cells. Biochem Biophys Res Commun 305:534–540. doi:10.1016/S0006291X(03)00794-0

Wain AR (2011) Patterns of growth and culturing protocols for *Salpingoeca rosetta* to be used in investigations of the origin of animal multicellularity. University of Akron (Master's thesis)

Weibel DB, Diluzio WR, Whitesides GM (2007) Microfabrication meets microbiology. Nat Rev Microbiol 5:209–218. doi:10.1038/nrmicro1616

Xia Y, Rogers JA, Paul KE, Whitesides GM (1999) Unconventional methods for fabricating and patterning nanostructures. Chem Rev Columb 99:1823–1848. doi:10.1016/j.chroma.2007.05.064

Zheng S, Lin H, Liu J, Balic M, Datar R, Cote RJ, Tai Y (2007) Membrane microfilter device for selective capture, electrolysis and genomic analysis of human circulating tumor cells. J Chromatogr A 1162:154–161. doi:10.1016/j.chroma.2007.05.064